Solid-State Multinuclear NMR Studies of Ferroelectric, Piezoelectric, and Related Materials

Steven F. Dec, Mark F. Davis, Gary E. Maciel,* and Charles E. Bronnimann‡

Department of Chemistry, Colorado State University, Fort Collins, Colorado 80523

John J. Fitzgerald* and Sang-sub Han

Department of Chemistry, South Dakota State University, Brookings, South Dakota 57007

Received February 19, 1992

High-field ^{47}Ti and ^{49}Ti, ^{67}Zn, ^{91}Zr, and ^{137}Ba magic-angle-spinning NMR spectra are reported for the following ferroelectric, piezoelectric, and related materials: $SrTiO_3$, $BaTiO_3$, $CaTiO_3$, TiO_2, $BaZrO_3$, $SrZrO_3$, BaO, ZnO, and ZnS. The observed line shapes are rationalized in terms of the local symmetry of the various metal atom sites. An indication of the sensitivity of chemical shifts of the various metal cations to local chemical structure is given. In addition, ^1H CRAMPS NMR spectra of some zirconium and titanium salts that are used as precursors in the production of electrical materials are discussed.

Introduction

A wide array of ferroelectric, piezoelectric, and pyroelectric materials have titanium, zirconium, and zinc metal cations as part of their elemental composition.[1-4] Many electrical materials based on titanium oxide (titanates) and zirconium oxide (zirconates) are known to have structures based on perovskite-type oxide lattices.[1-4] Barium titanate, $BaTiO_3$, and a diverse compositional range of PZT materials (lead zirconate titanates, $Pb_xZr_yTi_{1-y}O_3$) and PLZT materials (lead lanthanum zirconate titanates, $Pb_xLa_{1-x}Zr_yTi_{1-y}O_3$) are among these perovskite-type electrical materials.[1-4] Some materials containing the zinc cation, such as ZnO and ZnS, are also piezoelectric.[4] The structural characterization of the barium, titanium, zirconium, and zinc cation sites in these types of materials would aid our understanding of their chemical and physical properties, and multinuclear NMR should be helpful in this regard.

The synthesis of various metal oxide ceramics often employs solid-state reactions that involve the thermal decomposition of metal hydroxide and metal chelate precursors or the use of metal alkoxide sol–gel precursors.[5-10] In particular, PZT and PLZT ceramics have been synthesized from solid-state reactions of oxides or carbonates of the metal cations and from solutions containing $ZrOCl_2 \cdot 8H_2O$ and $TiOSO_4$.[8,9] In addition to a knowledge of the metal cation chemistry, the structural characterization of the hydrogen atom chemistry of metal oxide precursor materials would be of use in helping to develop and understand synthetic pathways for the production of electrical materials, and ^1H NMR should be useful in this context.

For the study of these types of materials by solid-state NMR, even the most favorable of the NMR-active nuclides of barium, titanium, zirconium, and zinc (^{137}Ba, ^{47}Ti and ^{49}Ti, ^{91}Zr and ^{67}Zn) are expected to exhibit low sensitivity; each of these nuclides has a moderately large nuclear electric quadrupole moment, eQ,[11] and a small magnetogyric ratio.[12] The relatively recent developments of very high-field (14.1 T) solid-state NMR of metal nuclides,[13] as well as the recent developments of dynamic-angle-spinning (DAS)[14] and double-rotation (DOR)[15] techniques, should facilitate the study of the above-mentioned materials. In solid-state ^1H NMR, strong homonuclear dipolar coupling can obscure the chemical shift fine structure expected for systems that contain protons in chemically distinct sites. However, the technique of combined rotation and multiple-pulse spectroscopy (CRAMPS)[16] for high-resolution solid-state ^1H NMR may provide a useful ^1H NMR approach for the systems of interest. A summary of the parameters of interest in the NMR of these nuclides is given in Table I.

While a substantial number of ^1H CRAMPS studies have recently appeared,[16-23] only a small number of solid-state NMR studies concerned with quadrupolar metal nuclides of low magnetogyric ratio, especially the nuclides of interest in this paper, have been published. Kunwar and co-workers[24] have observed

* To whom correspondence should be addressed.

‡ Present address: Chemagnetics, Inc., 2555 Midpoint Dr., Fort Collins, CO 80525.

(1) Jaffe, B.; Cook, W. R.; Jaffe, H. *Piezoelectric Ceramics*; Academic Press: London, 1979.
(2) Buchanan, R., Ed. *Ceramic Materials for Electronics*; Marcel Dekker, Inc.: New York, 1986.
(3) Wakino, K. In *Fine Ceramics*; Saito, S., Ed.; Elsevier: New York, 1985; pp 251–261.
(4) West, A. R. *Basic Solid State Chemistry*; John Wiley and Sons: New York, 1988; pp 331–341.
(5) Amin, A.; Spears, M. A.; Kulwicki, B. M. *J. Am. Ceram. Soc.* **1983**, *66*, 733–738.
(6) Fang, T. T.; Lin, H. B. *J. Am. Ceram. Soc.* **1989**, *72*, 1899–1906.
(7) Hertl, W. *J. Am. Ceram. Soc.* **1988**, *71*, 879–883.
(8) Ritter, J. J.; Roth, R. S.; Blendell, J. E. *J. Am. Ceram. Soc.* **1986**, *69*, 155–162.
(9) Kezuka, K.; Hayashi, Y.; Yamaguchi, T. *J. Am. Ceram. Soc.* **1989**, *72*, 1660–1663.
(10) Haertling, G. H.; Land, C. E. *J. Am. Ceram. Soc.* **1971**, *54*, 1–11.
(11) Fuller, G. H. *J. Phys. Chem. Ref. Data* **1976**, *5*, 835–1092.
(12) Pople, J. A.; Schneider, W. G.; Bernstein, H. J. *High-Resolution Nuclear Magnetic Resonance*; McGraw-Hill Book Co.: New York, 1959; p 481.
(13) Dec, S. F.; Maciel, G. E. *J. Magn. Reson.* **1990**, *87*, 153–159.
(14) Mueller, K. T.; Sun, B. Q.; Chingas, G. C.; Zwanziger, J. W.; Terao, T.; Pines, A. *J. Magn. Reson.* **1990**, *86*, 470–487.
(15) Samoson, A.; Lippmaa, E.; Pines, A. *Mol. Phys.* **1988**, *65*, 1013–1018.
(16) Maciel, G. E.; Bronnimann, C. E.; Hawkins, B. L. In *Advances in Magnetic Resonance: The Waugh Symposium, Vol. 14*; Warren, W. S., Ed.; Academic Press: New York, 1990; pp 125–150.
(17) Rosenberger, H.; Ernst, H.; Scheler, G.; Juenger, I.; Sonnenberger, R. *Z. Phys. Chem.* **1982**, *263*, 846–848.
(18) Rosenberger, H.; Scheler, G.; Buerger, H.; Jakob, M. *Colloids Surf.* **1984**, *12*, 53–58.
(19) Gerstein, B. C.; Chow, C.; Pembleton, R. G.; Wilson, R. C. *J. Phys. Chem.* **1977**, *81*, 565–570.
(20) Bronnimann, C. E.; Zeigler, R. C.; Maciel, G. E. *J. Am. Chem. Soc.* **1988**, *110*, 2023–2026.
(21) Bronnimann, C. E.; Hawkins, B. L.; Zhang, M.; Maciel, G. E. *Anal. Chem.* **1988**, *66*, 1743–1750.
(22) Jurkiewicz, A.; Bronnimann, C. E.; Maciel, G. E. *Fuel* **1990**, *69*, 804–809.
(23) Jurkiewicz, A.; Bronnimann, C. E.; Maciel, G. E. *Fuel* **1989**, *68*, 872–876.
(24) Kunwar, A. C.; Turner, G. L.; Oldfield, E. *J. Magn. Reson.* **1986**, *69*, 124–127.

0020-1669/93/1332-0955$04.00/0

Table I. ^{47}Ti, ^{49}Ti, ^{67}Zn, ^{91}Zr, and ^{137}Ba NMR Parameters

nuclide	ν_0 (MHz)[a]	I[b]	Q (barn)[b]	natural abund (%)[c]
^{47}Ti	33.8	$^5/_2$	0.29	7.75
^{49}Ti	33.8	$^7/_2$	0.24	5.51
^{67}Zn	37.5	$^5/_2$	0.16	4.12
^{91}Zr	55.8	$^5/_2$		11.23
^{137}Ba	66.7	$^3/_2$	0.28	11.32

[a] Resonance frequency, ν_0, at 14.1 T. Reference 12. [b] Reference 11. [c] Reference 12.

^{67}Zn in a sample of zinc acetate and Forbes and co-workers[25] have used variable-temperature solid-state NMR to record ^{137}Ba and ^{47}Ti and ^{49}Ti spectra of $BaTiO_3$ above its Curie temperature. The most extensive study of the metal cations of interest in this paper is that of Hartman and co-workers,[26] who reported ^{91}Zr NMR spectra of $BaZrO_3$, $SrZrO_3$, and a number of different samples of partially stabilized zirconia.

The discussion of the materials of interest in this paper is based on the measured NMR parameters of these materials under ambient-temperature and -pressure conditions. These NMR parameters can, in general, be expected to be dependent on temperature and/or pressure variations. For example, Forbes and co-workers[26] were able to observe ^{137}Ba and ^{47}Ti and ^{49}Ti resonances of $BaTiO_3$ only above its Curie Temperature, where $BaTiO_3$ has a cubic structure. Variable-temperature NMR and variable-pressure NMR experiments should prove to be useful in future studies of these materials.

In this paper, we report ^{47}Ti, ^{49}Ti, ^{67}Zn, ^{91}Zr, and ^{137}Ba NMR results obtained at high field, using magic-angle spinning (MAS), for a number of samples that are of interest in the electronics industry. For some samples, spectra were obtained as a function of external magnetic field strength in order to determine the contribution of quadrupolar effects to the observed spectra. ^1H CRAMPS spectra are also reported for a number of hydroxyl-containing complexes of titanium and zirconium.

Experimental Section

Materials. Commercially available samples of $CaTiO_3$ (Alfa Products, Johnson Matthey), $SrTiO_3$ (Alfa Products, Johnson Matthey), $BaTiO_3$ (AESAR/Johnson Matthey), $SrZrO_3$ (Alfa Products, Johnson Matthey), $BaZrO_3$ (Alfa Products, Johnson Matthey), BaO (Barco Products), ZnO (J. T. Baker Chemical Co.), ZnS (Fisher Scientific Co.), anatase TiO_2 (Aldrich Chemical Co., Inc.), $TiOSO_4 \cdot xH_2SO_4 \cdot xH_2O$ (Aldrich Chemical Co., Inc.), $Zr(SO_4)_2 \cdot 4H_2O$ (Alfa Products, Johnson Matthey), and powdered $ZrO(OH)(CO_3)_{0.5}$ (Magnesium Elektron, Inc.) were obtained from the indicated sources and used as received. Crystals of $ZrOCl_2 \cdot 8H_2O$ were provided by Prof. Abraham Clearfield (Texas A&M University).

NMR Measurements. Solid-state $^{47}Ti/^{49}Ti$, ^{67}Zn, ^{91}Zr, and ^{137}Ba MAS NMR spectra were recorded on Bruker AM-500 (11.7 T) and AM-600 (14.1 T) NMR spectrometers using home-built MAS probes. Torlon spinners (9-mm outer diameter, ~0.4-cm^3 sample volume), capable of MAS speeds of 4–6 kHz, were used to record the spectra. A pulse sequence of the Hahn-echo type[24] was used to record the spectra in order to eliminate artifacts due to transmitter and probe circuit "ringing". The external (substitution) chemical shift references, all assigned to 0 ppm, are the ^{49}Ti resonance of neat $TiCl_4(l)$, the ^{67}Zn resonance of 0.1 M $ZnCl_2(aq)$, and the ^{137}Ba and ^{91}Zr resonances of solid $BaZrO_3$. Spectra were obtained with pulse repetition delays of 1–5 s and from addition of 5000–100,000 transients. Corrections for the field-dependent second-order quadrupolar frequency shifts that are, in general, observed for quadrupolar nuclei in noncubic environments[27,28] have not been applied in some cases in this paper. In such cases, only "apparent chemical shifts" have been determined from the $^{47}Ti/^{49}Ti$, ^{67}Zn, ^{91}Zr, and ^{137}Ba MAS NMR spectra.

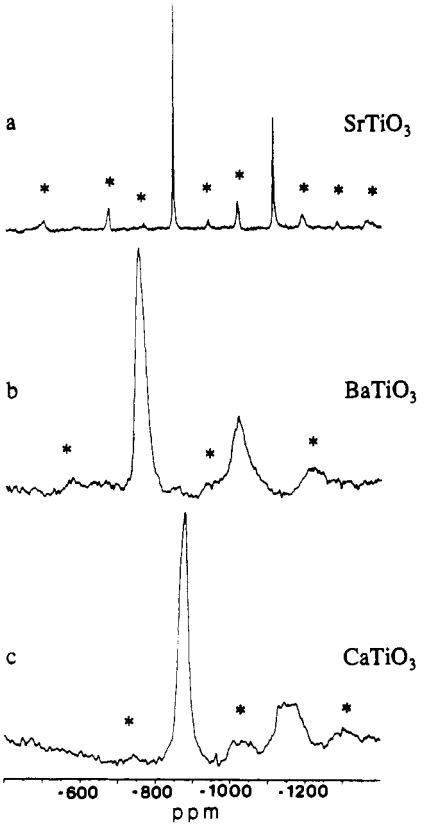

Figure 1. 14.1-T ^{47}Ti and ^{49}Ti MAS NMR spectra of (a) $SrTiO_3$, (b) $BaTiO_3$, and (c) $CaTiO_3$. Asterisks indicate spinning sidebands.

^1H CRAMPS NMR spectra (187 MHz) were recorded on a severely modified Nicolet NT-200 NMR spectrometer, with a home-built probe based on a Gay-type[29] MAS system, using the BR-24 pulse sequence.[30] The chemical shift reference was external tetrakis(trimethylsilyl)methane (TTMSM), with a peak at 0.38 ppm relative to liquid tetramethylsilane (TMS); ^1H chemical shifts are reported relative to liquid TMS.

Results and Discussion

Figure 1 shows 14.1-T ^{47}Ti and ^{49}Ti MAS NMR spectra of $SrTiO_3$, $BaTiO_3$, and $CaTiO_3$. Titanium has six nearest-neighbor oxygen atoms in these titanates.[31] The influence of the second cation in these titanates on the ^{47}Ti and ^{49}Ti peak positions, as well as the effect of the symmetry of the titanium sites on the line shapes, is evident from the spectra.

The ^{47}Ti and ^{49}Ti MAS NMR spectrum of cubic $SrTiO_3$,[31] presented in Figure 1a, shows the expected result for a titanium site with local octahedral symmetry. Both the ^{47}Ti and ^{49}Ti resonance lines are very sharp, because there is no contribution to the observed NMR spectrum from quadrupolar effects for quadrupolar nuclei in sites with cubic symmetry.[27,28] The two isotropic peaks observed in the titanium MAS NMR spectrum of $SrTiO_3$ are assigned to the ^{47}Ti and ^{49}Ti nuclides on the basis of the known values of their magnetogyric ratios.[12] Since the ^{49}Ti nuclide has a larger magnetogyric ratio than that of the ^{47}Ti nuclide, the isotropic peak positions of −843 and −1110 ppm (both referred to the ^{49}Ti resonance of $TiCl_4(l)$) are assigned to the ^{49}Ti nuclide and the ^{47}Ti nuclide, respectively.

In contrast to the titanium NMR spectrum of $SrTiO_3$, the ^{47}Ti and ^{49}Ti MAS NMR spectra of $BaTiO_3$ (Figure 1b) and $CaTiO_3$ (Figure 1c) exhibit broader resonance lines. This is expected, because the titanium sites in these samples do not have cubic symmetry, and second-order quadrupole effects appear in the

(25) Forbes, C. E.; Hammond, W. B.; Cipollini, N. E.; Lynch, J. F. *J. Chem. Soc., Chem. Commun.* **1987**, 433–436.
(26) Hartman, J. S.; Koffyberg, F. P.; Ripmeester, J. A. *J. Magn. Reson.* **1991**, *91*, 400–404.
(27) Kundla, E.; Samoson, A.; Lippmaa, E. *Chem. Phys. Lett.* **1981**, *83*, 229–232.
(28) Ganapathy, S.; Schramm, S.; Oldfield, E. *J. Chem. Phys.* **1982**, *77*, 4360–4365.
(29) Gay, I. D. *J. Magn. Reson.* **1984**, *58*, 413–420.
(30) Burum, D. P.; Rhim, W.-K. *J. Chem. Phys.* **1979**, *71*, 944–956.
(31) Wells, A. F. *Structural Inorganic Chemistry*, 5th ed.; Clarendon Press: Oxford, England, 1984; pp 584–588.

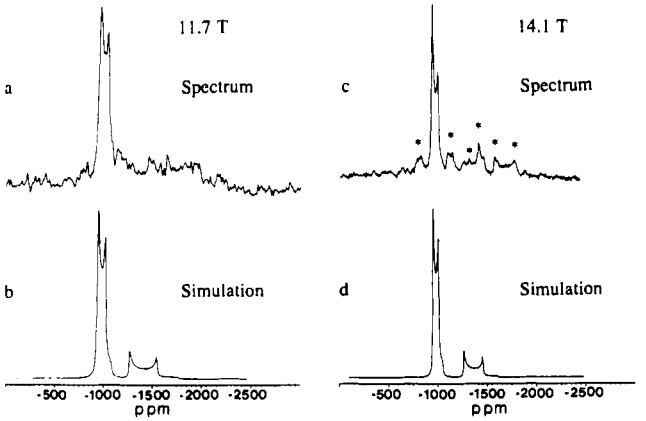

Figure 2. (a) 11.7-T ^{47}Ti and ^{49}Ti MAS NMR spectrum of anatase, TiO_2. (b) Simulation of (a). (c) 14.1-T ^{47}Ti and ^{49}Ti MAS NMR spectrum of anatase. (d) Simulation of (c). Asterisks indicate spinning sidebands.

MAS spectra.[27,28] $BaTiO_3$ has a tetragonal structure,[31] and $CaTiO_3$ has an orthorhombic structure;[32] the titanium cation in each sample is displaced from the center of the octahedron defined by its six nearest-neighbor oxygen atoms. For $BaTiO_3$, the ^{47}Ti and ^{49}Ti peak positions ("apparent chemical shifts") in the spectrum obtained at 14.1 T are about −1040 and −746 ppm, respectively, both relative to the ^{49}Ti peak of $TiCl_4$(l). Similarly, for $CaTiO_3$ the ^{47}Ti and ^{49}Ti peak positions observed at 14.1 T are about −1160 and −874 ppm, respectively. For both $BaTiO_3$ and $CaTiO_3$, the ^{47}Ti peaks are broader than the ^{49}Ti resonance peaks. Second-order quadrupole effects are expected[27,28] to make a larger contribution to the ^{47}Ti line shape than for the ^{49}Ti peak, because the ^{47}Ti nuclide has a larger quadrupole moment and a smaller spin ($^5/_2$) than the ^{49}Ti nuclide ($^7/_2$).[11]

The titanium MAS NMR spectra of $SrTiO_3$, $BaTiO_3$, and $CaTiO_3$ show that the non-titanium cation in these titanates has a relatively large effect on the ^{47}Ti and ^{49}Ti chemical shifts. For these particular titanates the ^{47}Ti and ^{49}Ti chemical shift range is on the order of 100 ppm.

Figure 2 shows ^{47}Ti and ^{49}Ti MAS NMR spectra obtained at 11.7 and 14.1 T on the anatase form of TiO_2.[33] At both magnetic field strengths, the ^{47}Ti/^{49}Ti spectrum is dominated by an intense feature in the frequency range of about −900 to −1100 ppm. A broader and less well-defined pattern of resonance intensity can be seen at lower frequency than the dominant feature. Both patterns are observed to narrow, with the intensity maxima shifting to higher frequency, as the static magnetic field strength is increased from 11.7 to 14.1 T. This feature, which is much more evident for the dominant pattern, is identified as a MAS-averaged second-order quadrupolar powder pattern, because it exhibits the field dependence predicted by theory[27,28] for a resonance line that has this effect as its major source of line shape. The dominant (higher frequency) pattern is most probably due to the ^{49}Ti nuclide, because the ^{49}Ti nuclide has a smaller quadrupole moment and larger spin than the ^{47}Ti nuclide and has, therefore, smaller contributions to its observed NMR line shape from second-order quadrupole effects.[27,28] The broader, lower-frequency pattern, which is much more apparent in the 14.1-T spectrum than in the 11.7-T spectrum, is assigned to ^{47}Ti. Parts b and d of Figure 2 show simulations of the spectra at 11.7 and 14.1 T based on the assignment of the feature between −900 and −1100 ppm to the MAS-averaged ^{49}Ti resonance of TiO_2 under the second-order quadrupole effect.[27,28] At 11.7 and 14.1 T, the simulations give isotropic chemical shifts of −916 and −920 ppm, respectively (a modest discrepancy between values that should be identical), a

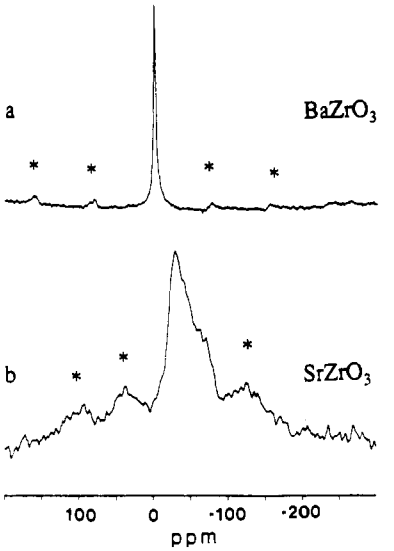

Figure 3. 14.1-T ^{91}Zr MAS NMR spectra of (a) $BaZrO_3$ and (b) $SrZrO_3$. Asterisks indicate spinning sidebands.

quadrupole coupling constant, e^2qQ/h, of 4.6 MHz, and an asymmetry parameter, η, of zero. This value of η indicates that the titanium cation site in anatase has axial symmetry, in agreement with the known structure of anatase, where the local symmetry of the titanium site is D_{4h} because there are two equivalent, axial Ti–O bond lengths of 1.980 Å and four equivalent, equatorial Ti–O bond lengths of 1.934 Å.[33]

The ^{47}Ti resonances in the 11.7- and 14.1-T MAS NMR spectra of anatase (Figure 2a,c) are not nearly as distinct as the ^{49}Ti resonance lines. However, the expected position and line shape of the ^{47}Ti resonance line can be calculated from the ^{49}Ti results and used to assign some of the features in the 14.1-T spectrum of anatase (Figure 2c). The simulation of the ^{47}Ti resonance line of anatase is shown in the −1200 to −1650 ppm spectral region of the 14.1-T spectrum (Figure 2d) and the −1200 to −1800 ppm region of the 11.7-T spectrum (Figure 2c). The position of the ^{47}Ti resonance pattern in the simulation is based on the 267 ppm difference in resonance line position between the ^{47}Ti and ^{49}Ti nuclides measured in the ^{47}Ti and ^{49}Ti MAS NMR spectrum of $SrTiO_3$ (Figure 1a). Each titanium nucleus in anatase has the same electric field gradient tensor, and thus the ^{47}Ti resonance line has the same eq and η values as those of ^{49}Ti. The ^{47}Ti MAS-averaged second-order quadrupolar pattern[27,28] spans a larger frequency range than that of the ^{49}Ti nuclide, because the ^{47}Ti nuclide has a larger quadrupole moment and smaller spin than the ^{49}Ti nuclide. The simulation of the 14.1-T ^{47}Ti MAS NMR spectrum permits the peaks at −1252 and −1457 ppm to be assigned to the horns of the MAS-averaged second-order quadrupolar powder pattern. Other features of the ^{47}Ti resonance line in the 14.1-T MAS NMR spectrum are not apparent, presumably because the MAS speed, 5.3 kHz, is too small to place spinning sidebands from both the ^{47}Ti and ^{49}Ti resonance lines outside the spectral region spanned by the ^{47}Ti resonance pattern.

Figure 3 shows 14.1-T ^{91}Zr MAS NMR spectra obtained on the zirconates, $BaZrO_3$ and $SrZrO_3$. These spectra agree well with the lower-field ^{91}Zr MAS NMR spectrum of $BaZrO_3$ and the static-sample ^{91}Zr NMR spectrum of $SrZrO_3$ reported by Hartman and co-workers.[26] The ^{91}Zr MAS NMR spectrum of cubic $BaZrO_3$[34] (Figure 3a) has a very sharp peak, because the zirconium site in this sample has local octahedral symmetry; this peak is suitable as a ^{91}Zr chemical shift reference and, hence, was assigned a chemical shift of 0 ppm. In contrast, the ^{91}Zr MAS

(32) Koopmans, H. J. A.; Van de Velde, G. M. H.; Gellings, P. J. *Acta Crystallogr.* **1983**, *C39*, 1323–1325.
(33) Reference 31, p 541.
(34) Scholder, R.; Raede, D.; Schwarz, H. *Z. Anorg. Allg. Chem.* **1968**, *362*, 149–168.

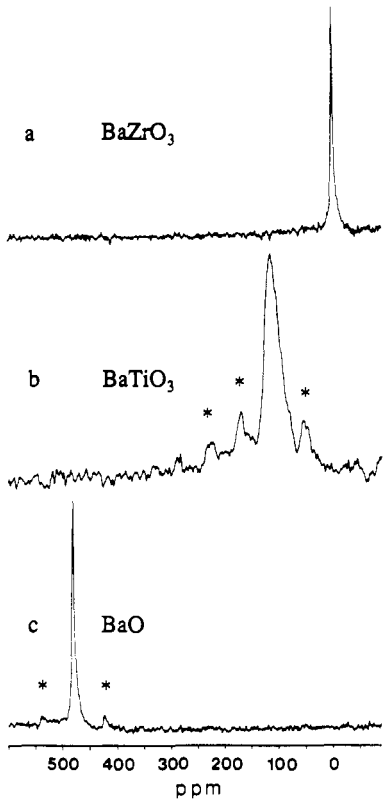

Figure 4. 14.1-T ^{137}Ba MAS NMR spectra of (a) $BaZrO_3$, (b) $BaTiO_3$, and (c) BaO. Asterisks indicate spinning sidebands.

NMR spectrum of orthorhombic $SrZrO_3$[35] has a much broader resonance (peak width on the order of 50 ppm) with an *apparent* chemical shift at 14.1 T of about −30 ppm. The ^{91}Zr resonance line of $SrZrO_3$ is expected to be substantially broad, because the position of the zirconium nucleus is not at the center of the octahedron defined by its six nearest-neighbor oxygen atoms.[35] The contribution of quadrupole effects to the ^{91}Zr MAS NMR spectrum of $SrZrO_3$ is difficulat to assess quantitatively. The characteristic discontinuities of a MAS-averaged second-order quadrupolar powder pattern,[27,28] which may be obscured by a significant contribution from the dispersion of isotropic chemical shifts of chemically different zirconium sites, are not apparent in the ^{91}Zr spectrum of $SrZrO_3$. Also, note that the substitution of strontium for barium in these zirconates has a relatively small effect on the *apparent* ^{91}Zr chemical shifts; this indicates that ^{91}Zr NMR for zirconates may not be as sensitive to local structural variations as ^{47}Ti/^{49}Ti NMR is for the analogous titanates, where a larger chemical shift range is observed (Figure 1).

Figure 4 shows 14.1-T ^{137}Ba MAS NMR spectra obtained on $BaZrO_3$, $BaTiO_3$, and BaO. The spectrum of cubic $BaZrO_3$[34] (Figure 4a) consists of a sharp line, because the barium site has local octahedral symmetry, which provides a convenient ^{137}Ba chemical shift reference. Hence, this species is assigned a chemical shift of 0 ppm. In contrast, the ^{137}Ba MAS NMR spectrum of tetragonal $BaTiO_3$,[31] with an *apparent* chemical shift of 115 ppm at 14.1 T, has a relatively broad resonance line, presumably due to significant contributions from second-order quadrupole effects;[27,28] the barium nucleus is displaced from the center of the cuboctahedron defined by its twelve nearest-neighbor oxygen atoms. The ^{137}Ba MAS NMR spectrum of cubic BaO[36] also consists of a sharp resonance, because the barium site has local octahedral symmetry and second-order quadrupole effects do not affect its NMR spectrum;[27,28] the isotropic chemical shift is 481 ppm. In addition to the effect of the local barium symmetry

(35) Carlsson, L. *Acta Crystallogr.* **1967**, *23*, 901–905.
(36) Reference 31, p 537.

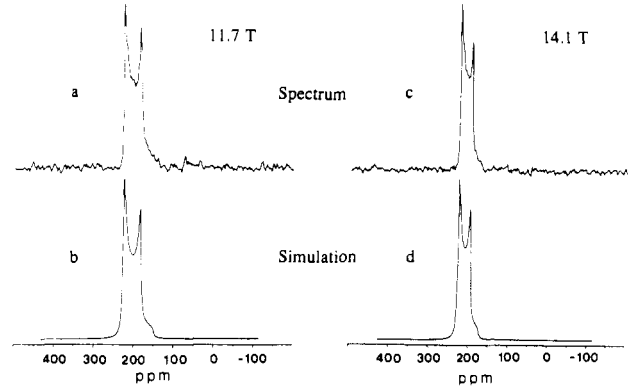

Figure 5. ^{67}Zn MAS NMR spectra of ZnO: (a) spectrum at 11.7 T; (b) simulation of (a); (c) spectrum at 14.1 T; (d) simulation of (c).

on the observed line shapes in the ^{137}Ba spectra, these ^{137}Ba MAS NMR spectra also illustrate the effect of the local barium chemical environment on the observed ^{137}Ba chemical shifts. A ^{137}Ba chemical shift change of about 400 ppm is observed between BaO, in which barium has six nearest-neighbor oxygen atoms, and $BaTiO_3$ or $BaZrO_3$, in both of which barium has twelve nearest-neighbor oxygen atoms. Replacement of zirconium by titanium in the six-coordinate sites of the perovskite-type oxide lattices of $BaZrO_3$ and $BaTiO_3$ also lowers the shielding of the ^{137}Ba nucleus by about 100 ppm.

Figure 5 shows 11.7- and 14.1-T ^{67}Zn MAS NMR spectra obtained on ZnO. The complex line shape is observed to narrow, with the intensity maxima shifting to higher frequency as the external field is increased from 11.7 to 14.1 T, indicating that the dominant cause of the line shape is the second-order quadrupole effect.[27,28] Simulation of the MAS-averaged quadrupolar powder patterns[27,28] gives good agreement for the two static magnetic fields applied, yielding an isotropic chemical shift of 239 ppm, $e^2qQ/h = 2.4$ MHz, and $\eta = 0$ at 14.1 T and an isotropic chemical shift of 237 ppm, $e^2qQ/h = 2.4$ MHz, and $\eta = 0$ at 11.7 T. This value of η indicates that the zinc site in ZnO has axial symmetry, a result in agreement with the known wurtzite-type crystal structure of ZnO, with hexagonal symmetry.[37,38] The zinc site in ZnO has four nearest-neighbor oxygen atoms, with one unique Zn–O bond distance and three equivalent Zn–O bond distances; thus, the zinc site in ZnO has a local axially symmetric C_{3v} symmetry, which is manifested as $\eta = 0$.

Figure 6 shows 11.7- and 14.1-T ^{67}Zn MAS NMR spectra of ZnS. Two peaks are observed, with intensity maxima at 378 and 360 ppm, positions that are independent (in ppm) of field strength. This behavior[27,28] indicates that these two peaks correspond to isotropic ^{67}Zn NMR chemical shifts of two different zinc sites in ZnS. The stable forms of ZnS, in which each zinc cation has four nearest-neighbor sulfur atoms, are known to be the cubic zinc blende structure and the hexagonal wurtzite structure.[39] The zinc site has local tetrahedral symmetry in the zinc blende form of ZnS[40] and should have a ^{67}Zn NMR peak position that is independent of external field because quadrupole effects do not contribute to the NMR spectrum of a nuclide with cubic symmetry.[27,28] In contrast to ZnO, the wurtzite structural form of ZnS has a nearly ideal wurtzite structure.[40] This implies that all four Zn–S linkages in the wurtzite form of ZnS are equivalent and that the local zinc cation symmetry is tetrahedral; therefore, it is expected that the ^{67}Zn MAS NMR peak position of the wurtzite form of ZnS should also be independent of the applied external field. Thus, the two peaks observed in the ^{67}Zn MAS

(37) Abrahams, S. C.; Bernstein, J. L. *Acta Crystallogr.* **1969**, *B25*, 1233–1236.
(38) Sabine, T. M.; Hogg, S. *Acta Crystallogr.* **1969**, *B25*, 2254–2256.
(39) Cooper, M. J.; Rouse, K. D.; Fuess, H. *Acta Crystallogr.* **1973**, *A29*, 49–56.
(40) Reference 4, pp 27–44.

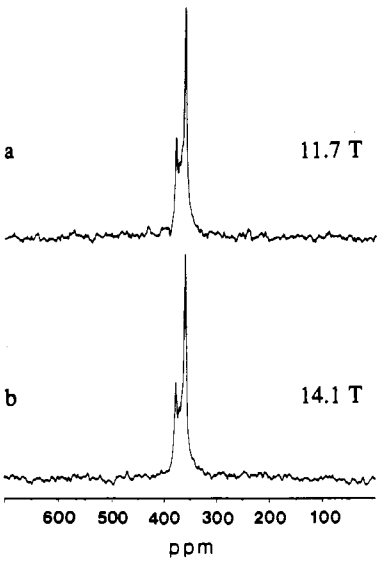

Figure 6. ^{67}Zn MAS NMR spectra of ZnS: (a) 11.7 T; (b) 14.1 T.

NMR spectrum of ZnS correspond to the zinc sites of the two stable forms of ZnS. Because the local zinc structure in these two forms of ZnS is very similar,[40] it is not possible at this time to assign a particular peak in the ^{67}Zn MAS NMR spectrum to one of the forms of ZnS.

Figure 7 shows ^{1}H CRAMPS NMR spectra obtained on a number of titanium and zirconium salts. In some cases, the spectra yield a wealth of structural information. The spectrum of the extensively hydrolyzed, gelatinous complex $ZrO(OH)(CO_3)_{0.5}$[41] (Figure 6a) shows only a single peak centered at 5.7 ppm, the width of which is probably due to a range of chemically distinct Zr–OH moieties. The ^{1}H CRAMPS spectrum of $ZrOCl_2{\cdot}8H_2O$ (Figure 6b) exhibits two peaks centered at 7.1 and 9.5 ppm (appearing as a shoulder). The structure of $ZrOCl_2{\cdot}8H_2O$ is based on the tetrameric $Zr_4(OH)_8(H_2O)_{16}^{8+}$ cation that has a $Zr–OH_2$:Zr–OH ratio of 4:1;[42] thus, on the basis of the relative peak intensities observed in the ^{1}H CRAMPS spectrum of $ZrOCl_2{\cdot}8H_2O$, the peaks with chemical shifts of 7.1 and 9.5 ppm are assigned to the $Zr–OH_2$ and Zr–OH protons, respectively.

The spectrum of $Zr(SO_4)_2{\cdot}4H_2O$ (Figure 6c) shows a single, sharp resonance line with a chemical shift of 8.8 ppm. $Zr(SO_4)_2{\cdot}4H_2O$ has a chain-type structure in which the zirconium atoms are bridged by hydroxyl groups.[43] The ^{1}H CRAMPS spectrum indicates that all of the bridging hydroxyl groups are chemically equivalent.

The ^{1}H CRAMPS spectrum of $TiOSO_4{\cdot}xH_2SO_4{\cdot}xH_2O$ (Figure 6d) shows three distinct peaks and one shoulder, all in the 5–10 ppm region. This material probably contains a number of structurally distinct Ti–OH, Ti–OH–Ti, and $Ti–OH_2$ moieties.

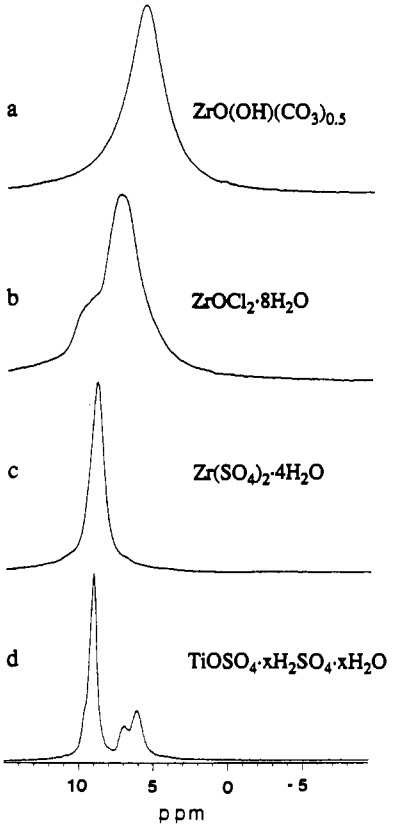

Figure 7. ^{1}H CRAMPS NMR spectra of (a) $ZrO(OH)(CO_3)_{0.5}$, (b) $ZrOCl_2{\cdot}8H_2O$, (c) $Zr(SO_4)_2{\cdot}4H_2O$, and (d) $TiOSO_4{\cdot}xH_2SO_4{\cdot}xH_2O$.

In conclusion, the results reported in this study indicate that $^{47}Ti/^{49}Ti$, ^{67}Zn, ^{91}Zr, and ^{137}Ba MAS NMR techniques are not limited to the study of materials that have cubic symmetry and that useful structural information can be obtained from samples with lower symmetry. Except perhaps for ^{91}Zr, all of the metal nuclides have chemical shifts that are relatively sensitive to their local chemical structure. In addition, the quadrupolar parameters, e^2qQ/h and η, should be useful for obtaining structural information on the metal cation sites in electrical materials. ^{1}H CRAMPS NMR spectra of the titanium and zirconium salts reported in this work show that chemically distinct proton sites can be resolved and that ^{1}H CRAMPS should prove useful for the study of the chemistry involved in the production of electrical materials.

In those cases in which large quadrupole coupling constants (e^2qQ/h) lead to broad second-order quadrupolar patterns even at 14.1 T, DAS[14] and/or DOR[15] techniques may prove valuable. In such cases, the present paper should provide useful background data.

Acknowledgment. We acknowledge use of the Colorado State University NMR Center and partial support by NSF Grant No. CHE-9021003.

(41) Blumenthal, W. B. *The Chemical Behavior of Zirconium*; Van Nostrand: New York, 1958.
(42) Clearfield, A.; Vaughan, P. A. *Acta Crystallogr.* **1956**, *9*, 555–558.
(43) Singer, J.; Cromer, D. T. *Acta Crystallogr.* **1959**, *12*, 719–723.